

# EFFECTS OF QUENCHING-MEDIUM ON THE CRYSTAL STRUCTURE OF ASSAB-CORAX STEEL

Aziz K. Jahja and Nurdin Effendi

Research and Development Centre for Materials Science and Technology  
National Nuclear Energy Agency  
Kawasan Puspiptek, Serpong, Tangerang 15314

## ABSTRACT

**EFFECTS OF QUENCHING-MEDIUM ON THE CRYSTAL STRUCTURE OF ASSAB-CORAX STEEL.** X-ray diffraction experiment was carried out on commercial Assab-Corax steel sample. The samples were quenched after heat-treated at 920 °C in three different media, air, water and brine. The main objective was to check on any significant changes occurring in the crystal-structure of the sample, before tempering could be carried out. The x-ray diffraction intensity was collected using the step counting method with a 0.05° stepscan and 2 seconds preset time. The refinement was carried out using the  $Im3m$  model, and the results show that the Carbon atoms are distributed among the base position in the body centered cubic unit cell at the eight-fold octahedral interstitial sites. It was verified that although there is a slight expansion in the lattice parameter due to lattice distortion effected by the carbon atoms and a variation in terms of relative peak intensities and the FWHM values, no fundamental structural changes have taken place after the 920 °C pre-tempering heat-treatment. It was found that alloys quenched in a brine medium, have the best chance to conserve both the crystalline structure and the hardness property of the original untreated sample. The highest hardness value is from the brine-quenched medium at  $(373 \pm 4)$  HVN which lies within the experimental error of the untreated sample's hardness  $(382 \pm 21)$  HVN. In the air- and brine quenched samples, the highest inhomogenous strain-field is in the  $[110]$  crystal direction, and is lowest in the  $[220]$  direction. Whereas for the water-quenched sample, these directions are the  $[310]$  and the  $[110]$  respectively.

**Key words :** Crystal structure, assab-corax steel, XRD, quenching-medium

## ABSTRAK

**PENGARUH QUENCHING-MEDIUM PADA STUKTUR KRISTAL BAJA ASSAB-CORAX.** Telah dilakukan eksperimen difraksi sinar-X pada sampel padatan Baja Assab-Corax komersial, untuk mempelajari struktur kristalnya. Sampel diquench setelah diberi perlakuan panas pada 920 °C dalam tiga media yang berbeda yaitu udara, air serta air garam. Tujuan utama dari penelitian ini adalah untuk mengetahui perubahan-perubahan yang terjadi jika ada, yang terjadi pada struktur kristal sebelum *tempering* dilakukan. Pengukuran dengan difraksi sinar-X dilakukan dengan menggunakan metode *step counting* dengan *step* 0,05°, dan waktu pencacahan 2 detik. Untuk analisis struktur dipilih model bcc dengan grup ruang  $Im3m$ , dan hasilnya menunjukkan bahwa atom-atom karbon terdistribusi secara interstisi dalam posisi dasar sel satuan kubik berpusat badan dengan posisi-posisi oktahedral simetri kelipatan delapan. Telah diverifikasi terjadinya pemuaian parameter kisi disebabkan distorsi kisi oleh atom-atom C, dan telah terjadi variasi pada intensitas puncak relatif dan nilai FWHM. Namun demikian tidak terdapat perubahan fundamental pada struktur kristal sesudah pemanasan pra-perlakuan *temper* pada 920 °C. Medium air-garam merupakan medium terbaik untuk *quenching* karena mampu mengkristalisasi paduan dengan lebih sempurna dan mempertahankan harga kekerasan sampel asli. Nilai kekerasan tertinggi ditunjukkan oleh sampel yang *diquench* dalam air-garam yaitu  $(373 \pm 4)$  HVN, masih dalam rentang galat eksperimental harga kekerasan sampel asli  $(382 \pm 21)$  HVN. Pada sampel yang *diquenching* di udara dan dalam air garam, nilai medan-regangan tak-homogen terdapat pada arah kristal  $[110]$ , nilai terendah pada arah  $[220]$ . Sedangkan untuk sampel yang *diquenching* di dalam medium air arah-arahnya masing-masing ialah  $[310]$  untuk yang tertinggi dan  $[110]$  untuk yang terendah.

**Kata kunci :** Struktur kristal, baja Assab-corrax, XRD, *quenching-medium*

## INTRODUCTION

Iron and Steel are one industrial commodity which have found the foremost industrial application among various materials. The economical value is determined by both the wide diversity in steel properties and the

ease of formability of steel products in general. Precisely this very high diversity in properties has made steel to have a highly attractive appeal to industrial manufacturers. One of the most important steel products

available in the current market is Assab-Corrax steel, a product of ASSAB STEEL Germany. In the general spec-sheet issued by the company, the steel is classified as plastic mould steel with high corrosion resistance and medium scratch capacity [1]. The chemical composition of this steel is tabulated in table 1.

Table 1. Chemical composition of Assab-Corrax steel [1]

Element	C	Cr	Mo	Mn	Si	Ni	Al
Content (at%)	0.03	12.30	1.40	0.03	0.30	9.2	1.6

The high Ni and Al contents are the reason why this type of steel is high-temperature resistant, and highly suitable for high temperature operations. The properties of steels, determined by dispersion strengthening, depend on the amount, size, shape and distribution of cementite. Quenching is one form of isothermal heat treatment, usually used in combination with other heat treatment such as tempering, for example to form martensite. Quench and temper heat treatments require the formation and decomposition of martensite, providing exceptionally fine dispersions of Fe<sub>3</sub>C. A quench and temper heat treatments provides a microstructure that can provide both strength and toughness. However no data or information is available on the behaviour of Assab steels in the post-quenching pre-tempering conditions. Therefore it is necessary to investigate the effect of quenching on the crystal structure of steels.

In this report, results of quenching in three different media, air, water and brine on the crystal structure of Assab-Corrax steel is reported. Using the Rietveld refinement method, the crystal structure of quenched samples is investigated, and the results compared to the untreated 'original' sample. The heat treatment temperature of 920 °C was chosen since it represents the temperature to prepare the sample for later tempering process [2]. Therefore the main objective of this work is in line with the long term objectives of this entire research work namely to gain complete understanding of Assab-Corrax crystal-structure especially with regard to the effects of quenching. The other motivation being its application as high-temperature component of nuclear power-plant turbine, located in the first zone (zone I) and extending out to the tertiary zone (zone III) of the power plant.

## THEORY

Low carbon steel goes through two allotropic transformations during heating or cooling. Immediately after solidification, low carbon steel forms a BCC structure called  $\delta$  -ferrite [3]. On further cooling the low carbon steel transforms to FCC structure called  $\gamma$ , or austenite-phase. Finally low carbon steel transforms back to BCC structure at lower temperatures; this structure is called  $\alpha$ - or ferrite-phase.

Both of the ferrite and the austenite are solid solutions of interstitial carbon atoms in low carbon steel. Especially, in the case of Assab-Corrax, the ferritic-phase is formed by addition of Cr-elements in order to facilitate the formation of the wider ferritic-phase and the ferritic-phase will be maintained down to room temperature. Because the interstitial holes in FCC lattice are somewhat larger than the holes in BCC lattice, a greater number of carbons atoms can be accommodated in FCC low carbon steels. Thus the maximum solubility of carbon in in BCC low carbon steel is much lower, ~ 0,0218 % in  $\alpha$  and 0,09 % in  $\delta$ . The solid solutions are relatively soft and ductile but are stronger than pure low carbon steel due to solid solution strengthening by the carbon. A stoichiometric compound Fe<sub>3</sub>C or cementite forms when the solubility of Carbon in solid low carbon steel is exceeded. The Fe<sub>3</sub>C contains 6,67% C, is extremely hard and brittle, and is present in all commercial steels. Thus by properly controlling the amount of Fe<sub>3</sub>C, the degree of dispersion strengthening and the property of steel could be controlled.

Quenching is one of the oldest method to increase the strength and hardness of steel. In  $\alpha$ -steels (ferrite) the C atoms is located on the edges of the cube, at the eightfold octahedral Wyckoff sites (8c). Therefore by quenching or rapid quenching, no Fe<sub>3</sub>C precipitate could be formed by insoluble C. The C remains in the lattice, but at the same time distorts the lattice simply, and this in turns could increase the strength and hardness of the steel, because the high stress induced during the samples' fabrication and heat treatment would block the propagation of the dislocation in the steel.

## EXPERIMENTAL

Assab-Corrax steel samples of German fabrication were obtained commercially from the market (P.T. Assab-Corrax Indonesia). The samples were cut into several pieces with dimension of 10 mm x 5 mm x 3 mm, and then polished using sand-paper with grids ranging from very coarse to very fine, i.e. 80, 100, 150, 200, 320, 400, 600, 800, 1000, 1500 and 2000 until the desired surface's smoothness is obtained and also in compliance with the standard protocols in x-ray diffraction measurements. All experimental work was carried out at BBI-P3IB laboratory. The polished samples are then heated to 920 °C which is the hardening temperature of the steel in order to dissociate existing carbide molecules in the sample and to free elements such as C or Cr to become free agents, with holding time of 24 hours. The heated samples are quenched from 920 °C in three different media, air, water and brine. The quenching was carried out manually, and therefore the quenching-rate could only be estimated at about 30 °C/s, if the time to take the sample out of the furnace is estimated to be around 30 s. The quenched samples are mounted by first adding resin as a glue-material and then put in the

XRD-sample holder before exposure to the radiation of the x-ray diffraction apparatus. Diffraction intensity was measured using the P3IB-BATAN Shimadzu X-Ray Diffractometer, by step counting method with a 0.05° step-scan and the preset time of 2 seconds.

Using the collected experimental data the background, the scale-factor and phase-dependent parameters were refined using the least-squares method of the Rietan programme [4]. Hardness test was performed separately on the samples using the macro hardness tester Vickers method (VHN).

## RESULT AND DISCUSSION

### Hardness Test

In table 2 the results of the hardness test using the Vickers method on the four samples (one untreated sample and three quenched samples) is presented.

Table 2. Hardness Test Data on the Assab-Corax Steel. The number in the parentheses show the standard deviation value

Sample	Hardness Test Number			Average Hardness (kgf/mm <sup>2</sup> )
	1 (kgf/mm <sup>2</sup> )	2 (kgf/mm <sup>2</sup> )	3 (kgf/mm <sup>2</sup> )	
untreated	371	407	371	382
Brine	371	378	371	373
Water	330	336	330	332
air	306	301	306	304

It is obvious that the highest hardness value is maintained by the sample quenched in brine (average hardness value of 373 VHN). This is because of the brine's physical property, namely heat conductivity, is higher for brine ( $k = 0.13 \text{ W/mK}$ ) than for water ( $k = 0.08 \text{ W/mK}$ ) and air ( $k = 0.05 \times 10^{-8} \text{ W/mK}$ ) [5]. And therefore the working cooling rate or the amount of heat transferred into the quenching-medium (in this case brine) is larger when compared to the two other media, and so it is expected that very little amount of internal stresses would build-up inside the quenched samples' bulk.

### Crystal Structure Investigation

In figure 1 the continuous counting diffraction pattern of untreated Assab-Corax sample is presented. From figure 1 the unit cell parameters are calculated using the nominal wavelength of the x-ray diffraction and the results compared to the literature [6]. The experimental parameters will be used as the initial (guessed) input parameters in the Rietveld refinement procedures. It was evident from the initial (manual) analysis of the cell parameters that the crystal structure of the sample phase is based on a body-centered-cubic (bcc) unit cell. In table 3. Structural parameters of the untreated Assab-Corax sample is presented.

It is evident from the results of X-ray diffraction continuous counting experiment in figure 1 that the

sample, in both the untreated and the heat-treated condition, is in the ferrite (single) phase and has a body-centered-cubic structure, so it is preferred to employ the bcc structure model represented by the  $Im\bar{3}m$  space group. Therefore in the refinement process it was assumed that in both conditions (pre-quenched and quenched), the sample has the same phase, i.e. crystallographically modeled using the bcc structure model, with the C atoms positioned at interstitial octahedral sites. The refinement of the structural parameters using x-ray diffraction intensity is carried out by employing the specially developed computer application code *RIETAN* attributed to F. Izumi [4]. *Pseudo-Voigt* profile function and conjugate-direction iteration method were used in the refinement process. It turns out that the conjugate direction method requires a much longer computing-time, however it ensures a better convergence if compared to the Marquardt method. Refined parameters include global parameters, background- and shift parameters, and phase-dependent parameters, in this case preferred orientation, lattice parameter and isotropic thermal factor.

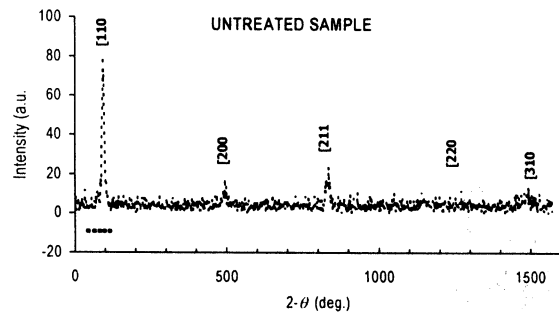


Figure 1. Continuous counting diffraction pattern of untreated Assab-Corax sample. The  $[hkl]$  numbers of each peak are indicated on top of each peak.

Table 3. Structural parameters of Assab-Corax Steel

(hkl)	Relative $I_0$ (counts)	FWHM
(110)	165568	0.640
(200)	29067	0.3795
(211)	38706	0.5312
(220)	15613	1.0393
(310)	32097	1.9995

$$a = 2.79(3) \text{ \AA}; Q = 1.0 (8) \text{ \AA}^2;$$

C content at the Wyckoff (8c) position in the unit cell = 0.012 at.%

Results of Rietveld refinement are presented in figures 2, 3 and 4 respectively. The observed, the calculated (refined) intensity and the refinement residuals are presented for the three quenching conditions.

The refinement results are shown in table-4. The lattice parameter  $a$  and isotropic temperature factor  $B$

are shown with the reliability indices (R factors). The lattice parameter and the temperature factor in all three quenching media agree within the range of statistical errors (standard deviation), although the sample

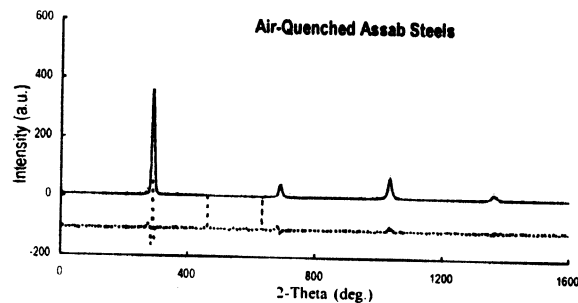


Figure 2. Refined diffraction pattern of Assab-Corrax steel quenched in air. Observed intensity (♦), calculated intensity (solid lines) and residuals ( $\sigma$ )

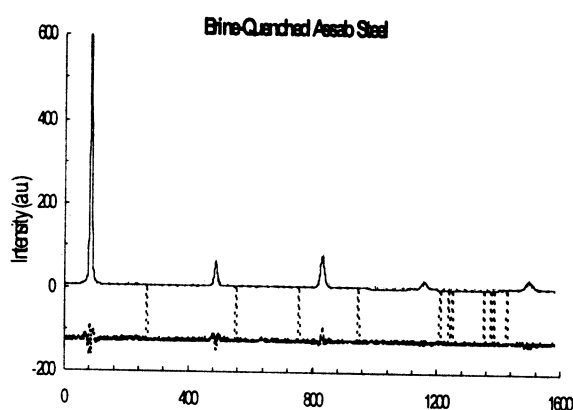


Figure 3. Refined diffraction pattern of Assab-Corrax steel quenched in brine

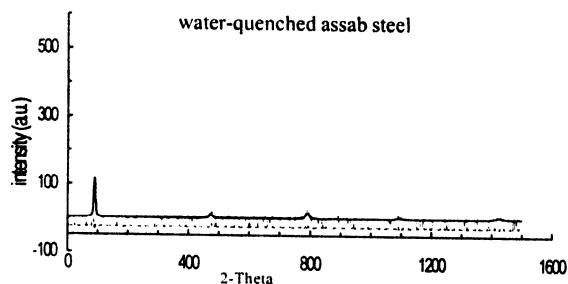


Figure 4. Refined diffraction pattern of Assab-Corrax steel quenched in water

quenched in brine shows a higher carbon content than the other two and approaching the value of maximum carbon content given in the spec-sheet of the company, therefore quenching, and especially brine-quenching managed to retain the carbon atoms inside the unit-cell and no  $Fe_3C$  intensity was observed in the diffraction pattern. Compared to the untreated sample, a slight increase in the lattice parameter  $a$  is observed, indicating a slight distortion in the lattice because of the carbon atoms inside the lattice attempting to diffuse out of the lattice and also due to the fact that thermal expansion had begun to set in and was arrested by the quenching process. But there is a possibility that free C-atoms had also managed to diffuse into the ferrite unit cell.

### Strain-Field Analysis

When a sample is subjected to homogenous strain, the peaks angular position will shift to either lower or higher  $2\theta$  values, subject to whether a *yield*- or a *tensile*-strain is being applied on the sample. On the other hand an *inhomogenous* strain field will cause besides an angular shift also a broadening in the intensity profile. The shift in peak-position is tied to the average strain in the crystals direction. The peak-broadening reveals information on the inhomogenous strain-field distribution fluctuation [5].

The average lattice strain in the crystal direction  $[hkl]$ , is expressed by:

$$\varepsilon_{hkl} = \frac{d - d_0}{d_0}$$

Here  $d$  and  $d_0$  are stress-free and stress-induced lattice-distance respectively. In table 5, the  $\varepsilon_{hkl}$  and  $d_{hkl}$  values for each quenching-phase are presented and compared.

Comparison of the relative intensity and the FWHM measures of the major peaks is shown in table 6. It is evident that there are considerable differences in the relative peak intensities for different samples quenched in different medium. And also there have been changes in the relative intensity if compared to the untreated sample. Judging from the intensity and FWHM measures, the brine-quenched sample seems

Table 4. Refined structural Parameters of Assab-Corrax based alloy (quenched after 920 °C heat-treatment in various media).

Phase <sup>*)</sup> M (Fe-Ni-Cr)	Lattice parameter $a$ (Å) <sup>**)</sup>	$Q$ (Å <sup>2</sup> )	$R_{wp}$ (%)	$R_p$ (%)	$R_F$ (%)	$R_I$ (%)	"Goodness of Fit S"	Carbon content (at.%)
Quench- condition								
Water	2.877 (3)	0.9 (2)	45.25	36.21	20.11	29.6	0.92	0.013(2)
Air	2.876 (1)	1.3 (4)	36.81	27.58	7.76	12.28	1.18	0.012(8)
Brine	2.883 (2)	0.8 (1)	34.73	24.10	6.42	9.46	1.14	0.031(7)

\*) An imaginary chemical species M(Fe-Ni-Cr) was input.

\*\*) Numbers in parentheses indicate standard deviation in the last significant digit of refined parameters.  
 SG.  $Im\bar{3}m$  (vol. I-229) : 1601 data points, 5 reflections (110), (200), (211), (220) and (310).

Table 5. Comparison of  $\epsilon_{hkl}$  and  $d_{hkl}$  values for each quenching-phase.\*

Untreated		Air		Water		Brine	
[hkl]	$d_{hkl,0}$ (Å)	$d_{hkl}$ (Å)	$\epsilon_{hkl}$	$d_{hkl}$ (Å)	$\epsilon_{hkl}$	$d_{hkl}$ (Å)	$\epsilon_{hkl}$
110	1.97171	2.03970	0.03448	2.0360	0.03166	2.03414	0.03166
200	1.39421	1.44228	0.03448	1.43868	0.03190	1.43835	0.03166
211	1.13837	1.17762	0.03448	1.17468	0.03190	1.17441	0.03166
220	0.98585	1.01985	0.03449	1.01730	0.03190	1.01707	0.03167
310	0.88178	0.91218	0.03448	0.90990	0.03189	0.90969	0.03165
Average			0.03448(0)		0.03185(1)		0.03166(1)

\*) The number inside parentheses indicates the uncertainty of the last significant digit

Table 6. Comparison of Relative Intensity of Major Peaks and FWHM of the ferrite M(Fe-Ni-Cr) phase

(hkl)	Relative $I_o$ (counts) Air quenched	FWHM	Relative $I_o$ (counts) Water quenched	FWHM	Relative $I_o$ (counts) Brine quenched	FWHM
(110)	100000	0.3324	100000	0.3106	100000	0.4069
(200)	16043	0.4550	28415	0.5677	18545	0.4113
(211)	31896	0.6306	43745	0.8498	28219	0.4487
(220)	12016	0.8740	26685	1.2037	10381	0.5532
(310)	9980	1.2538	19770	1.7315	7527	0.8073

to retain the perfect crystalline structure compared to the other two, since it has the smallest FWHM values, also an indication that microstrain and crystallite size could be reduced in the brine-quenched sample. Calculation of the average  $\epsilon_{hkl}$  values show that the air-quenched sample has the highest value and the brine-quenched sample has the lowest value.

The profile-broadening induced by inhomogenous strain-field  $e^2_{hkl}$  is expressed by :

$$B^2 = B_o^2 + 32 \ln 2 e^2_{hkl} (\tan \theta)^2 \quad (2)$$

$B$  is the FWHM of peak-broadening and  $B_o$  is the angular dependent instrument resolution, given by the Cagliotti expression [7] as follows,

$$B_o^2 = U_o (\tan \theta)^2 + V_o (\tan \theta) + W_o \quad (3)$$

$U_o$ ,  $V_o$ , and  $W_o$  are the three Gaussian FWHM parameters. Using the RIETAN-refined values of  $U_o$ ,  $V_o$ , and  $W_o$ , both  $B_o$  and the inhomogenous strain field  $e_{hkl}$  could be calculated from equations (2) and (3). In table 7, the values of the inhomogenous strain field  $e_{hkl}$  are presented.

Table 7. Inhomogenous strain-field  $e_{hkl}$

[hkl]	$e_{hkl}$ (%)		
	Air	Water	Brine
[110]	0.23596	0.14910	0.20191
[200]	0.19457	0.18117	0.12416
[211]	0.18501	0.19993	0.09225
[220]	0.18391	0.21331	0.08204
[310]	0.18651	0.22445	0.08963

In the air- and brine quenched samples, the highest inhomogenous strain-field is in the [110] crystal direction, and is lowest in the [220] direction. Whereas

for the water-quenched sample, these directions are the [310] and the [110] respectively.

## CONCLUSION

The crystal structure of the Assab-Corax stainless steel is preferably the body centered cubic (bcc) model, crystallographically represented by the  $Im\bar{3}m$  space group. Refinement results show that the C atoms are distributed among the eight-fold interstitial octahedral position in the face centered cubic unit cell by substitution mechanism. No crystallographic changes have been observed in the sample after heat treatment at 920 °C, and also in preparation for tempering. No  $Fe_3C$  intensity has been observed in the quenched samples, the C atoms are still distributed in the bcc unit cell. The brine-quenched sample evidently shows a better promise to maintain the crystalline structure and the hardness property of the samples before tempering is carried out on the samples. Therefore brine should be recommended as a preferable quenching medium for the pre-tempering heat treatment of this type of steels. It is concluded that no fundamental changes with respect to crystalline structure took place after the heat treatment especially in the brine-quenched sample, and the ferrite-phase is still maintained by the Assab-Corax based alloy.

## ACKNOWLEDGEMENT

The authors would like to express their gratitude to Drs. Gunandjar, S.U., Director of P3IB-BATAN, for his valuable support and for suggesting this project, so that this programme could be carried out. Gratitude is also due to Mr. Drs. Bambang H. Pranowo, project manager for the 2003 fiscal year at P3IB-BATAN for the financial support.

## REFERENCES

- [1]. *Assab-Corrax General Specification Sheet*, Assab-Corrax GmbH (2003)
- [2]. ARTHUR F. FOSTER and ROBERT R. WRIGHT JR., *Basic Nuclear Engineering*, Allyn and Bacon Inc., Boston, London, Sydney, second edition (1975).
- [3]. ASM Vol. 3, *Alloy Phase Diagram*, The Mater. Information Soc., (1990)
- [4]. F. IZUMI, *The Rietan Programme*, F. Izumi, J. Mineral Soc. Japan **17** (1985) 37
- [5]. B. ADJANTORO, *Jurnal Konduktor Padat*, **5**(1), (2004) 21-28
- [6]. P. VILLARS and L.D. CALVERT, *Pearson's Handbook of Crystallographic Data for Intermetallic Phases 2<sup>nd</sup> ed.*, **2B**, ASM International (1991).
- [7]. CAGLIOTI, G., PAOLETTI, A. and RICCI, F. P., *Nucl. Instrum. Methods*, **3** (1958) 223